Collision-induced electronic transitions

D. Rogovin
Rockwell International Science Center, Thousand Oaks, California 91360
(Received 7 March 1985)

We examine collision-induced electronic transitions mediated via long-range electrostatic fields such as those generated by ions and molecular dipoles. The chief characteristics of such processes are the relatively narrow widths and intense strengths of the collision-induced spectral lines. These features arise from and reflect the long-range nature of electrostatic forces which tend to generate long-lived collision-induced transition electric dipole moments. Of particular interest is the prediction that the collision-induced electromagnetic rates are proportional to the Raman cross section of the normally forbidden transition.

I. INTRODUCTION

Collision-induced (CI) absorption has long been of interest to the fields of atomic and molecular spectroscopy.[1-3] To date, research has been devoted to collision-induced nonelectronic transitions, in particular, translational, rotational, and vibrational transitions mediated by both short- and long-range intermolecular forces. For example, the far-infrared spectrum of H_2 arising from collision-induced translational absorption has been observed in detail by Kiss *et al.*[4] and Bosomworth and Gush,[5] whereas Kiss and Welsh[6] have examined the collision-induced rotational spectrum of H_2 and H_2—rare-gas mixtures. Furthermore, numerous workers[6-8] have observed pressure-induced absorption for the fundamental band of hydrogen in H_2, H_2—rare-gas, H_2-N_2, and H_2-O_2 mixtures. These CI spectra are all induced by either short-range or multipolar forces utilizing neutral particles as perturbers. More recently, several workers have observed collision-induced vibrational transitions in the solid hydrogens utilizing charged particles[9] as perturbers.

In sharp contrast, the phenomena discussed in this paper are based on the notion of inducing a transient electric dipole moment on a normally forbidden electronic transition. Specifically, we examine collision-induced electronic transitions due to long-range electrostatic forces such as those associated with neutral plasmas and molecular dipoles in un-ionized gases.[10,11] As in all CI processes, these forces distort the electronic structure of the atom (we will always refer to the absorber or emitter as the atom) and this distortion is responsible for the formation of a CI transition electric dipole moment which lasts as long as the system is perturbed. In turn, this CI transient dipole provides a mechanism for electric dipole emission or absorption on the forbidden electronic transition. Here, we examine the electrodynamic characteristics associated with collision-induced radiation processes on an electronic transition arising from long-range, electrostatic forces, specifically those generated by ions in a neutral plasma and by molecular dipoles in un-ionized gases. We calculate the collision-induced absorption experienced by a weak probe field which is swept across the CI spectral line. We also evaluate the collision-induced spontaneous emission rate of a collection of excited atoms which are exposed to perturbers. Before outlining the material contained in this paper, we briefly summarize our results.

Theoretical calculations reported in this paper assert that the ion-atom collision-induced absorption coefficient $\alpha_1(\omega)$ is given by

$$\alpha_1(\omega)=\frac{8\pi}{27}(Ze\lambda)^2\frac{c}{v_T}\ln\left[\frac{\lambda_D}{b^*}\right]\times\left[\frac{\partial}{\partial\omega'}\sigma_R(\omega,\omega')\right]_{\omega'=0}\mathscr{L}_1(\Delta\omega,T)n_pN\ . \tag{1.1}$$

In Eq. (1.1), Ze is the ion's charge, $\lambda(\omega)$ the photon wavelength (frequency), v_T the relative thermal velocity of a colliding ion-atom pair, λ_D the plasma Debye wavelength, b^* the hard-core impact parameter, $\sigma_R(\omega,\omega')$ the Raman cross section on the forbidden transition for processes in which a photon of frequency $\omega(\omega+\omega')$ is absorbed (emitted), $\mathscr{L}_i(\Delta\omega,T)$ the line shape at a frequency $\Delta\omega$ away from line center, n_p the ion density, and N the atomic density. The logarithmic factor arises from the long-range nature of the ion-atom interaction and the n_p factor reflects our assumption that different collisions give uncorrelated contributions to CI absorption. The presence of the Raman scattering cross section can be understood as follows. The collision-induced electronic transitions discussed in this paper are a two-step process which involves a virtually excited intermediate state. This state is connected to both the initial and final states of the atom by allowed electric dipole transitions. Since both steps of the process proceed via an allowed electric dipole transition, it is not surprising that the Raman cross section enters into the CI absorption coefficient. The width of the collision-induced spectral lines is determined by the inverse of the collision time which is the range of the force divided by the collision velocity. Due to the long-range nature of these forces, especially those associated with neutral plasmas, typical linewidths are on the order of tens of wave numbers rather than hundreds of wave numbers characteristic of CI infrared spectra. Further-

more, the collision-induced spectral line shape for electronic transitions $\mathscr{L}_1(\Delta\omega,T)$ is the same as the inelastic rotational scattering cross section of a molecular dipole with an ion. The underlying physics responsible for this fact is that for CI processes the electric field of the ion couples to the electrical dipole moment operator of the atom, whereas for inelastic rotational scattering the electric field of the ion couples to the rotational dipole moment operator of the molecule[12] so that both processes involve the same interaction. It is also worth noting that CI electronic transitions that are due to long-range forces are much more intense than collision-induced spectral lines due to short-range intermolecular interactions. These typically require several atmospheres of gas to obtain observable infrared spectra; in contrast, ion-atom collision-induced electronic spectra should be experimentally observable for gas densities of well under a torr. Typical values for the ion-atom collision-induced absorption coefficient, on resonance, are on the order of a few tenths of a percent per torr of absorber for a few tenths of a torr of perturber.

The relative velocity of the colliding particles influences the line width, line shape, and intensity of the ion-atom collision-induced electronic spectral lines. Specifically, the lower the relative velocity, the narrower are the spectral lines and the greater is the absorption near line center. If the collision velocity is reduced even further, as in a merging beam configuration, nonlinear electromagnetic effects may occur in the presence of intense, resonant laser radiation.[13] The physics of such situations will be discussed in future publications.

Finally, we note that collison-induced electronic transitions which proceed via a perturbing molecular dipole generally involve a shift in line position. This shift is equal to the level spacing between the two different perturber states that define the dipole and may involve a change in the perturber's rotational or rotovibrational state. Thus, significant shifts in the photon frequency may accompany collision-induced radiation processes. However, the most intense collision-induced transitions of this class of CI processes will be accomplished by molecules making a transition from the rotational state J to the states $J\pm1$. Hence, if the forbidden atomic transition is at ω_0, the most intense collision-induced spectral lines will appear at ω_0+2BJ and $\omega_0-2B(J+1)$, where B is the rotation constant of the molecule. Since a number of different rotational states are usually populated, it follows that the collision-induced spectral lines will appear centered at ω_0, $\omega_0\pm2B$, ω_0+4B, etc., their relative intensities being determined by the Boltzmann distribution for molecular rotators.

Collision-induced radiative phenomena arising from long-range electrostatic forces are discussed in Sec. II. We treat collision-induced radiative processes utilizing heavy particles, specifically ions and molecular dipoles, within the semiclassical Born approximation. More precisely, the center-of-mass motion of the colliding particles is regarded as classical in nature, whereas any changes in their internal state are treated quantum mechanically. General expressions are derived for the collision-induced electric dipole moment, absorption coefficient, and spontaneous emission rate arising from collisions between an atom and a perturber characterized by a multipole moment of order l_1. We apply this formalism in Sec. III where both ionic and molecular dipole perturbers are discussed. Finally, in Sec. IV we summarize our results and present our conclusions regarding collision-induced processes on forbidden electronic transitions due to long-range electrostatic forces.

II. FORMULATION OF THE PROBLEM

In this section we examine collision-induced radiative processes arising from long-range electrostatic forces such as those associated with ion-atom and dipole-atom interactions. In Sec. II A we derive expressions for various electromagnetic rates as well as the frequency-dependent absorption coefficient arising from a CI transient electric dipole moment. In Sec. II B we derive a general expression for the transient electric dipole moment due to collisions between a metastable atom and a heavy perturber which is characterized by an electric multipole moment of order l_1. Finally, in Sec. III C we construct the associated collision-induced spontaneous emission rate and absorption coefficient.

A. Electromagnetic rates

We first note that if a collision, occurring at a relative velocity v and impact parameter b, induces a transient electric dipole moment $\mathbf{p}(b,v,t)\exp(i\omega_{if}t)$ in an excited atom, then the energy $d\mathscr{E}_\omega$ radiated within a frequency interval ω to $\omega+d\omega$ about ω_{if} due to a single collision is,[14] from the Larmor relationship,

$$d\mathscr{E}_\omega=(2\omega^4/3\pi c^3)\,|\,\mathbf{p}(b,v,\omega)\,|^2 d\omega\ . \tag{2.1}$$

Here $\mathbf{p}(b,v,\omega)$ is the Fourier transform of $\mathbf{p}(b,v,t)$, ω_{if} refers to the frequency of the atomic transition, and the time dependence of $\mathbf{p}(b,v,t)$ arises from the relative motion of the perturber-atom pair. The total power $d\mathscr{P}_\omega$ emitted per radiator in the frequency interval ω to $\omega+d\omega$ is

$$d\mathscr{P}_\omega=2\pi\int_{b^*}^{\infty} db\, b\,\overline{\langle v\, d\mathscr{E}_\omega\rangle} n_p\ , \tag{2.2}$$

where the overbar implies a Boltzmann average over all initial atomic and perturber states as well as a sum over all final perturber and atomic states. The angular brackets imply a statistical average with a Boltzmann factor over the relative collision velocity, b^* is the hard-core impact parameter, and n_p is the perturber density. Physically, Eq. (2.2) states that the power radiated is just the energy emitted times the rate at which collisions occur, a consequence of our assumption that different collisions give uncorrelated contributions. Note that we are neglecting any contributions to the power arising from processes in which radiation emission is initiated by collisions with impact parameters less than b^*. For impact parameters on the order of or less than b^*, induced radiative processes arise from short-range interactions which are very large compared to k_BT and cannot be treated using first-order perturbation theory. However, we shall assume that their influence on the collision-induced radiative characteristics

of a normally forbidden electronic transition are quite small in comparison to electrostatic forces. The fact that most experiments involving collision-induced radiative phenomena that are mediated via short-range forces typically involve several hundred atmospheres of the gas of interest justifies this assumption.[2] In contrast, we shall consider situations involving only a few torr. Thus, to a first approximation in modeling the low-pressure collision-induced electronic transitions we shall neglect entirely events occurring for impact parameters less than b^*. We also note that there is a translational[3] contribution to the pressure-induced absorption. However, this occurs in the far infrared, that is, for frequencies on the order of $\hbar/k_B T$, which is much less than an atomic transition frequency and will be neglected. Inserting Eq. (2.1) into (2.2), we have for the power emitted per radiator in the frequency interval ω to $\omega+d\omega$

$$d\mathscr{P}_\omega=(4\omega^4/3c^3)n_p\int_{b^*}^{\infty}db\,b\langle v\overline{|\mathbf{p}(b,v,\omega)|^2}\rangle d\omega\ . \tag{2.3}$$

The collision-induced spontaneous emission rate at a frequency ω, $\mathscr{A}(\omega)$ is

$$\mathscr{A}(\omega)\equiv(d\mathscr{P}_\omega/d\omega)/\hbar\omega$$
$$=(4\omega^3/3\hbar c^3)\left[\int_{b^*}^{\infty}db\,b\langle v\,|\,\mathbf{p}(b,v,\omega)\,|^2\rangle\right]n_p \tag{2.4}$$

with the total rate over all frequencies being

$$A\equiv\int_0^\infty d\omega\,\mathscr{A}(\omega)\ . \tag{2.5}$$

If the density of atoms is N and they are all in the ground state, the collision-induced absorption coefficient $\alpha(\omega)$ is

$$\alpha(\omega)\equiv\frac{\lambda^2}{8\pi}N\mathscr{A}(\omega)=\frac{2\pi\omega}{3\hbar c}\int_{b^*}^{\infty}db\,b\langle v\overline{|\mathbf{p}(b,v,\omega)|^2}\rangle n_p N\ . \tag{2.6}$$

Next, we derive the cross section for collision-induced spontaneous emission, $\sigma^{i\to f}$. To calculate $\sigma^{i\to f}$, we require the probability that a perturber-atom collision, occurring at an impact parameter b, will give rise to photon emission. Thus, the probability that a photon of frequency ω is emitted during a collision with an impact parameter b is

$$\langle P_{i\to f}(\omega;b)\rangle=\frac{1}{\hbar^2}\left\langle\int_{-\infty}^{\infty}\overline{dt\,|\,\hat{\mathscr{T}}^{(2)}_{i\to f}(t)\,|^2}\rho(\omega)\right\rangle\ . \tag{2.7a}$$

Here, the outer angular brackets imply a statistical average and $\hat{\mathscr{T}}^{(2)}_{i\to f}(t)$ is the semiclassical matrix element for collision-induced emission processes, given by

$$\hat{\mathscr{T}}^{(2)}_{i\to f}(t)=\left\langle i\left|\hat{V}_C(t)\frac{1}{E_i-\hat{H}_0}\hat{V}_R+\hat{V}_R\frac{1}{E_i-\hat{H}_0}\hat{V}_C(t)\right|f\right\rangle\ . \tag{2.7b}$$

In Eq. (2.7b) the various operators are in the interaction representation, $\hat{V}_c$ is the long-range electrostatic interaction between the atom and perturber, $\hat{V}_R$ is the atomic dipole-field interaction for photons of frequency ω, $\hat{H}_0$ is the Hamiltonian of the isolated atom, and $\rho(\omega)$ is the photon density of states.

The differential cross section $\partial\sigma^{i\to f}/\partial\omega$ for the CI emission of a photon of frequency ω is

$$\frac{\partial\sigma^{i\to f}}{\partial\omega}=2\pi\int_{b^*}^{\infty}db\,b\langle P_{i\to f}(\omega;b)\rangle \tag{2.8}$$

and the total CI cross section is

$$\sigma^{i\to f}=2\pi\int_0^\infty d\omega\int_{b^*}^{\infty}db\,b\overline{\langle P_{i\to f}(\omega;b)\rangle}\ . \tag{2.9}$$

B. Collision-induced dipole moment

Next, we evaluate the collision-induced electric dipole moment arising from the long-range electrostatic interaction between an atom and a perturber possessing an electric multipole moment of order l_1. As noted in the Introduction, the long-range electrostatic field of the perturber will polarize the atom's electronic structure and this in turn will generate a CI transition electric dipole moment on the (normally) forbidden atomic transition. If the perturber has an electric multipole moment of order l_1, the specific interaction that is responsible for this polarization process is[15,16]

$$V_l(\mathbf{R})=-\frac{4\pi}{2l+1}\left[\frac{4\pi(2l+1)!}{3!(2l_1+1)!}\right]^{1/2}$$
$$\times\sum_{m,m_1m_2}\langle m_1m_2\,|\,l_m\rangle\mu^{l_1}_{m_1}(\hat{\mathbf{r}}_1)\mu^1_{m_2}(\hat{\mathbf{r}}_2)\frac{Y^*_{lm}(\hat{\mathbf{R}})}{R^{l+1}}\ , \tag{2.10}$$

where $\mathbf{R}\equiv R\hat{\mathbf{R}}$ is the center-of-mass separation, $\hat{\mathbf{r}}_1$ ($\hat{\mathbf{r}}_2$) refers to the internal coordinates of the perturber (atom), $\mu^{l_1}_{m_1}(\hat{\mathbf{r}}_1)=Q_{l_1}Y_{l_1m_1}(\hat{\mathbf{r}}_1)$ with Q_{l_1} the l_1 electric multipole moment operator of the perturber, $\mu^1_{m_2}(\hat{\mathbf{r}}_2)$ refers to the electric dipole moment operator of the atom, Y_{lm} is a spherical harmonic, $l=l_1+1$, and $\langle m_1m_2\,|\,lm\rangle$ is a Clebsch-Gordon coefficient. Thus, the long-range interaction can be regarded as a coupling between the perturber's multipole moment operator Q_{l_1} and the atom's electric dipole moment operator, which is analogous to near-resonant vibrational relaxation processes mediated by long-range electrostatic forces.[17] This is depicted in Fig. 1. Note that the optical excitation of the atom is virtual, as we are considering collision-induced processes on a forbidden transition, i.e., the matrix elements of $\mu^1_{m_2}(\hat{\mathbf{r}}_2)$ between the initial and final states of interest are zero. An examination of Eq. (2.10) reveals that the perturber may also change state, e.g., a molecular dipole perturber can switch its rotational, vibrational, or electronic state.

Since we are dealing with heavy colliding pairs interacting via a long-range, slowly varying electrostatic potential, it is sufficient to evaluate the various collision-induced processes to lowest order in $V_l(\mathbf{R})$ utilizing the semiclassical Born approximation. Since the relatively weak electrostatic forces give rise to only small angular deflections in the classical collision trajectories, the relative motion of the colliding particles is approximated by straight paths. We note that this approximation is no longer valid if orbiting occurs.

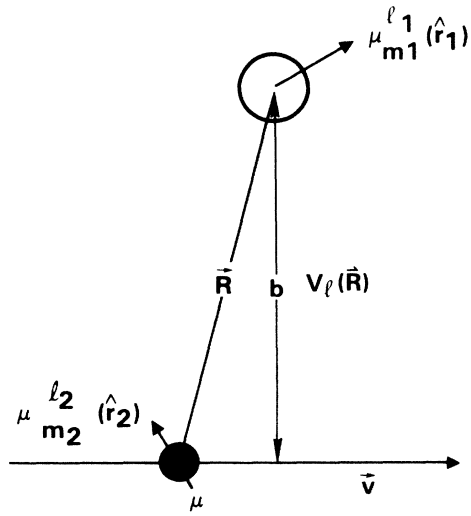

FIG. 1. Geometry of collision-induced dipole moment.

To calculate the collision-induced rates and spectra we require the Fourier transforms of the collision-induced transient electric dipole moment. To first order in $\hat{V}_l$, the CI transient electric dipole moment $p^{i\to f}_{m_3}(t)$ is given by

$$p^{i\to f}_{m_3}(t)=\frac{i}{\hbar}\int_{-\infty}^{t}dt'\langle f;a\,|\,[\mu^1_{m_3}(t),V_l(t')]\,|\,i;c\rangle\ , \tag{2.11}$$

where $|\,i;c\rangle$ ($|\,f;a\rangle$) denotes the initial (final) atomic and perturber states. The subindex m_3 refers to a particular component of the electric dipole moment operator. To evaluate the commutator in Eq. (2.11) we insert a complete set of atomic states, as we are considering only those processes in which the perturber does not form a chemical complex with the atom. If the intermediate atomic states are far removed from the forbidden transition so that $E_n-E_i(E_f)\gg\hbar v/b$, where E_n is the eigenenergy of the atomic state $|\,n\rangle$, v the relative velocity, and b the impact parameter, then

$$p^{i\to f}_{m_3}(b,t)=\frac{1}{\hbar}\sum_n\left[\frac{\langle f\,|\,\mu^1_{m_3}\,|\,n\rangle\langle n;a\,|\,\tilde{V}_l(t)\,|\,i;c\rangle}{\omega_{in}+\omega_{ac}}-\frac{\langle f;a\,|\,\tilde{V}_l(t)\,|\,n;c\rangle\langle n\,|\,\mu^1_{m_3}\,|\,i\rangle}{\omega_{nf}-\omega_{ac}}\right]\times e^{-i(\omega_{if}+\omega_{ac})t}\ , \tag{2.12}$$

where the time dependence of $\tilde{V}_l(t)$ arises from the classical relative motion of the perturber-atom pair. This time dependence governs the lifetime of the collision-induced electric dipole moment as well as the shape of the collision-induced spectral line. Figure 2 depicts the physical content of Eq. (2.12).

As noted above, long-range electrostatic forces are relatively weak, so that to a first approximation, we may assume straight paths for the collision trajectories and set

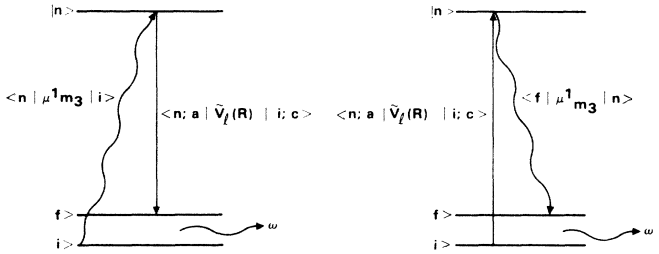

FIG. 2. Virtual process which gives rise to a collision-induced dipole moment.

$$R^2(t)=b^2+v^2t^2\ , \tag{2.13}$$

where b is the impact parameter.

Inserting Eq. (2.10) into Eq. (2.21), we obtain the following expression for the collision-induced dipole moment:

$$p^{i\to f}_{m_3}(t)=-\frac{4\pi}{2l+1}\left[\frac{4\pi(2l+1)!}{3(2l_1+1)!}\right]^{1/2}\times\sum_{mm_1m_2}\langle m_1m_2\,|\,l\rangle\langle\mu^{l_1}_{m_1}\,|\,c\rangle C^{i\to f}_{m_2m_3}\times\frac{Y^*_{lm}[R(t)]}{R^{l+1}(t)}\ , \tag{2.14}$$

where

$$C^{i\to f}_{m_2m_3}\equiv\sum_n\left[\frac{\langle f\,|\,\mu^1_{m_3}\,|\,n\rangle\langle n\,|\,\mu^1_{m_2}\,|\,i\rangle}{\omega_{nf}-\omega_{ac}}+\frac{\langle f\,|\,\mu^1_{m_2}\,|\,n\rangle\langle n\,|\,\mu^1_{m_3}\,|\,i\rangle}{\omega_{ni}+\omega_{ac}}\right] \tag{2.15}$$

is the scattering tensor for Raman processes[18] in which the atom, initially in the state $|\,i\rangle$, shifts a photon from ω_{if} to $\omega_{if}+\omega_{ac}$ and ends up in the state $|\,f\rangle$. An examination of Eq. (2.14) reveals that the collision-induced transition dipole $p^{i\to f}_{m_3}(t)$ reflects the anisotropic nature of long-range electrostatic forces via the spherical harmonic function $Y^*_{lm}[\hat{\mathbf{R}}(t)]$. Note that the ion-atom dipole for CI electronic transitions varies as $1/R^2$ which should be contrast with the CI induced dipole arising from the van der Waals interaction. This contains a short-range piece which exhibits an exponential dependence[19] on $R(t)$ as well as a component which varies as R^{-6} arising from the induced dipole-induced dipole interaction.

By Fourier transforming Eq. (2.14), we have for the collision-induced dipole moment oscillating at a frequency ω

$$p^{i\to f}_{l,m_3}(b,\omega)=B_l(v,b)\times\sum_{m_1m_2m}\langle m_1m_2\,|\,lm\rangle\times\langle a\,|\,\mu^{l_1}_{m_1}\,|\,c\rangle C^{i\to f}_{m_2m_3}f_{l,m}\left[\frac{\Delta\omega b}{v}\right]. \tag{2.16}$$

Here $\Delta\omega \equiv |\omega-\omega_{if}-\omega_{ac}|$,

$$B_l(v,b) \equiv -\frac{4\pi}{\sqrt{3}!}\frac{2^{l/2}(l+1)!}{\sqrt{(2l_1+1)!}}\frac{1}{vb^l}, \tag{2.17a}$$

and

$$f_{l,m}(x) \equiv \frac{(-1)^{l+m}}{2^{l/2}(l_1!)}\left[\frac{2l!}{(l-m)!(l+m)!}\right]^{1/2} x^l K_m(x), \tag{2.17b}$$

where $K_m(x)$ is a modified Bessel function or order m and argument x. Near line center, i.e., $x \to 0$,

$$f_{l,m}(x) \to \begin{cases} 0 & \text{if } m \neq \pm l \\ 2^l(l-1)! & \end{cases}, \tag{2.18}$$

whereas in the far wings of the line, i.e., $x \to \infty$,

$$f_{l,m}(x) \to \frac{(-1)^{l+m}}{2^{1/2}(l!)} \times \left[\frac{(2l)!}{(l-m)!(l+m)!}\right]^{1/2} x^{l-1/2}e^{-x}, \tag{2.19}$$

i.e., the Fourier transform of the CI dipole moment declines exponentially as $e^{-|\Delta\omega|b/v}$ for $|\Delta\omega| \gg v/b$.

C. Absorption coefficient

Having derived an expression for the collision-induced dipole moment, we can now construct the CI absorption coefficient $\alpha(\omega)$. To simplify matters, we shall assume that both the perturbers and the atoms are spatially homogeneous and in thermodynamic equilibrium at a temperature T. More specialized situations, such as those in which the particles collide in a beam configuration, are discussed separately in Sec. III.

To construct the CI absorption coefficient we require

$$S(\Delta\omega,b,v) \equiv \overline{\sum_{m_3} |p_{m_3}^{i\to f}|^2}, \tag{2.20}$$

which we refer to as the collision-induced optical strength function. The perturber states are denoted by $|n_pJ_pM_p\rangle$ and the atomic states by $|nJM\rangle$, where $J(J_p)$ and $M(M_p)$ refer to rotational quantum numbers and $n(n_p)$ to the remaining quantum numbers required to specify a particular quantum state. In the Appendix we show that

$$S_l(\Delta\omega,b,v) = \frac{B_l^2(v,b)\,|\langle n_pJ_p|Q_{l_1}|n_p'J_p'\rangle|^2\,|(n_iJ_i||T^{(k)}||n_fJ_f)|^2}{(2l_1+1)(2J_i+1)(2k+1)} L_l(\Delta\omega b/v), \tag{2.21}$$

where Q_{l_1} is the irreducible multipole moment of order l_1 of the perturber and

$$L_l(\Delta\omega b/v) \equiv \sum_m |f_{l,m}(\Delta\omega b/v)|^2 \tag{2.22}$$

is the first-order resonance function which determines the behavior of near-resonant, rotational multipole collisions. Thus, $l=3$ refers to dipole-quadrupole $l=2$ to dipole-dipole, and $l=1$ to dipole-monopole inelastic rotational collisions. The quantity $(n_iJ_i||T^{(k)}||n_fJ_f)$ is the irreducible Raman scattering tensor for electromagnetic processes of order k. Specifically, $k=2$ implies Raman processes in which $\Delta J = J_f - J_i = 2$, $k=1$ implies Raman processes in which $\Delta J = J_f - J_i = 1$, and $k=0$ implies Raman processes in which $J_f = J_i$, i.e., $\Delta J = 0$ transitions.

The collision-induced spontaneous emission rate $\mathscr{A}_l(\omega)$ at a frequency ω is

$$\mathscr{A}_l(\omega) = \frac{4\pi}{3}\frac{4\omega^3}{3\hbar c^3}\int_{b^*}^{b_l} db\, b\langle S_l(\Delta\omega,b,v)\rangle n_p, \tag{2.23}$$

where the upper limit of integration depends on the intermolecular force. If the perturber is characterized by a dipole or a higher-order multipole, then the collision-induced electric dipole moment converges sufficiently rapidly that b_l can be taken to be infinity. However, for radiative processes that are initiated by an ion, the long-range nature of the ion-atom force poses a convergence difficulty. In particular, for ion-atom processes the CI absorption coefficient will display a logarithmic singularity, and it is necessary to introduce a cutoff in Eq. (2.23) to obtain an acceptable description of ion-atom collision-induced processes. We note that in a neutral plasma the interaction between particles is characterized by the Debye screening length[20] λ_D. On physical grounds, we anticipate that the collision-induced dipole will drop off very rapidly for impact parameters $b \geq \lambda_D$ so that the cutoff parameter is the Debye length. Thus,

$$\mathscr{A}_l(\Delta\omega) = \frac{4\pi}{9}\frac{\overline{|\langle n_pJ_p|Q_{l_1}|n_p'J_p'\rangle|^2}}{2l_1+1} \times 4\pi\frac{\omega^3}{\hbar c^4}\frac{|(n_iJ_i||T^{(k)}_{\omega_{ac}}||n_fJ_f)|^2}{(2J_i+1)(2k+1)}n_p \times c\int_{b^*}^{b_l} db\, b^{1-2l}\left\langle\frac{1}{v}L_l(\Delta\omega b/v)\right\rangle, \tag{2.24}$$

where $b_l = \lambda_D$ if $l=1$ and is infinite otherwise. The quantity in angular brackets can be related to the Raman scattering cross section $\sigma_R^{i\to f}(\omega,\omega')$ defined by[17]

$$\sigma_R^{i\to f}(\omega,\omega') = 4\pi\frac{\omega'\omega^3}{\hbar c^4}\frac{|(n_iJ_i||T^{(k)}(\omega')||n_fJ_f)|^2}{(2J_i+1)(2k+1)}, \tag{2.25}$$

and since $\omega_{ac} \ll \omega$, we may write

$$\mathscr{A}_l(\Delta\omega) = \frac{4\pi}{9}n_p\frac{\overline{|\langle n_fJ_f|Q_{l_1}|n_iJ_i\rangle|^2}}{2l_1+1} \times \frac{\partial}{\partial\omega'}\sigma_R^{i\to f}(\omega;\omega')\Big|_{\omega'=\omega_{ac}} \times c\int_{b^*}^{b_l} db\langle vB_l^2(v,b)L_l(\Delta\omega b/v)\rangle \tag{2.26}$$

which is exact in the limit that $\omega_{ac} \to 0$. Finally, it is convenient to adopt a normalization condition such that the line-shape function $\mathscr{L}_l(\Delta\omega, T)$, defined below, is unity on resonance. Thus, for $l=1$, we have

$$Q_R(\omega,\omega') \equiv \frac{\partial \sigma_R}{\partial \omega'}(\omega,\omega') \,, \tag{2.27}$$

$$\mathscr{A}_1(\omega) = \frac{64\pi^2}{27}(Ze)^2 \frac{c}{v_T} Q_R(\omega,0) \ln\left[\frac{\lambda_\eta}{b^*}\right] n_p \mathscr{L}_1(\Delta\omega, T) \,,$$

where Ze is the ion's charge, v_T is the relative thermal velocity of the colliding pair, and

$$\mathscr{L}_1(\Delta\omega, T) \equiv \frac{v_T}{c} \int_1^{\lambda_D/b^*} \frac{dz}{z} \left\langle \frac{c}{v} L_1(\Delta\omega b^* z/v) \right\rangle \,. \tag{2.28}$$

For $l \geq 2$,

$$\mathscr{A}_l(\Delta\omega) = \frac{32\pi^2}{81} \frac{2^l (l-1)!}{(2l-1)(2L-1)!} \frac{c}{v_T} \times Q_r(\omega,\omega_{ac}) \frac{\bar{Q}_{l_1}^2}{(b^*)^{2(l-1)}} n_p \mathscr{L}_l(\Delta\omega, T) \,, \tag{2.29}$$

where it is understood that Eq. (2.29) is to be summed over all perturber transitions and

$$\mathscr{L}_l(\Delta\omega, T) \equiv v_T \int_1^\infty \frac{dz}{z^{2l-1}} \left\langle \frac{1}{v} L_l(\Delta\omega b^* z/v) \right\rangle \,. \tag{2.30}$$

If the density of atoms is N, all of which are in the ground state, then the frequency-dependent absorption coefficient is, for $l=1$,

$$\alpha_1(\omega) = \frac{8\pi}{27}(Ze\lambda)^2 \frac{c}{v_T} Q_R(\omega,0) \times [\ln(\lambda_D/b^*)] \mathscr{L}_1(\Delta\omega, T) n_p N \tag{2.31}$$

and, for $l \geq 2$,

$$\alpha_l(\omega) = \frac{4\pi^2}{81} \frac{2^l (l-1)!}{(2l-1)(2l-1)!} \frac{c}{v_T} \times \frac{\bar{Q}_{l_1}^2 \lambda^2}{(b^*)^{2(l-1)}} Q_R(\omega,\omega_{ac}) \mathscr{L}_l(\Delta\omega, T) n_p N \,. \tag{2.32}$$

III. APPLICATION TO IONS AND MOLECULAR DIPOLAR PERTURBERS

In this section we apply the formalism of Sec. II to treat the collision-induced electronic transitions utilizing (1) ions and (2) molecular dipoles in an un-ionized gas as perturbers. Ions are discussed in Sec. III A and molecular dipoles in Sec. III B.

A. Ionic perturbers

To eliminate any effects due to a net electrostatic field, we assume that the atoms of interest are immersed in an electron-ion charge neutral plasma. Due to their high thermal velocities, electrons do not significantly influence the CI electrodynamics of the atoms and therefore will be neglected. To investigate the role of anisotropy in collision-induced phenomena, we examine a spatially homogeneous plasma in Sec. III A 1 and discuss beam situations in Sec. III A 2.

1. Spatially homogeneous plasma

If the plasma is spatially homogeneous, then the formalism of Sec. II can be applied immediately to the problem. Figure 3 depicts the first-order resonance function for ion-atom collision-induced processes as a function of $\Delta\omega b/v \equiv \Delta\omega\tau$, where τ is a typical collision time. An examination of this figure reveals a well-defined dip at $\Delta\omega\tau = 0$ which arises from anisotropic forces. The full width at half maximum (FWHM) is on the order of 5 and beyond that the resonance function drops exponentially to zero as $\exp(-\Delta\omega\tau)$. Note that the CI optical strength function reflects the ion-atom interaction via the factor B_1^2 which varies with impact parameter as $1/b^2$.

The collision-induced spontaneous emission rate at a frequency ω is

$$\mathscr{A}_1(\omega) = \frac{64\pi^2}{27}(Ze)^2 \frac{c}{v_T} [\ln(\lambda_D/b^*)] \times Q_R(\omega_{if},0) n_p \mathscr{L}_1(\Delta\omega, T) \,, \tag{3.1}$$

where Ze is the ion's charge and $\mathscr{L}_1(\Delta\omega, T)$ is the collision-induced line shape. If the atoms are all in the ground state, then the frequency-dependent collision-induced absorption coefficient is

$$\alpha_1(\omega) = \frac{8\pi}{27}(Ze\lambda)^2 \frac{c}{v_T} \left[\ln\left[\frac{\lambda_D}{b^*}\right]\right] \times Q_R(\omega_{if},0) N n_p \mathscr{L}_1(\Delta\omega, T) \,. \tag{3.2}$$

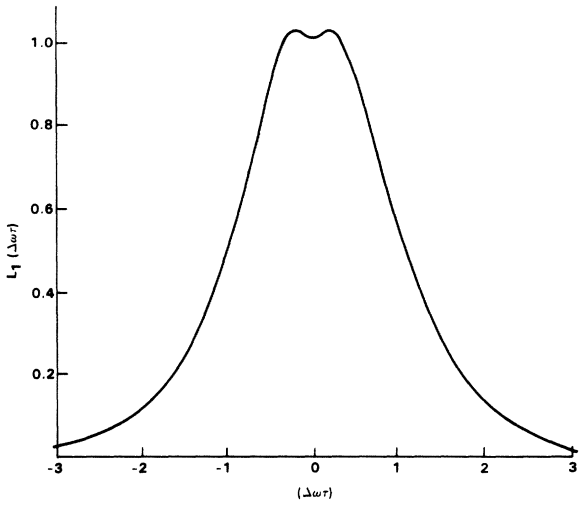

FIG. 3. First-order resonance function for ion-atom collision-induced absorption as a function of $\Delta\omega\tau$.

The absorption line-shape function $\mathscr{L}_1(\Delta\omega,T)$ is depicted in Fig. 4 for the case of Cs^+ as perturber and Sn as absorber at a temperature of 300 K with a hard-core impact parameter of 4 Å. The line-shape function, which is normalized to unit at line center, has the following characteristics: (1) it is relatively narrow with a linewidth (FWHM) on the order of 15 cm^{-1}; (2) it is symmetrical about line center; (3) for $\Delta\omega \gg v/b^*$ it declines exponentially, in fact, as $\exp(-\Delta\omega b^*/v)$; and (4) its shape and width are independent of gas pressure. Before commenting on these features we note that the dip at line center, although present in the first-order resonance function, will generally be washed out in any actual collision-induced spectral line shape. Specifically, in our approach the probability for a collision-induced transition has been cut off at the hard-core impact parameter because the intermolecular potential significantly changes from its multipolar form for $b \lesssim b^*$. For $b < b^*$, one might be tempted to assume that the probability for a collision-induced transition can be taken constant and equal to its value at b^*, in analogy with Gordon's[12] approach to rotational relaxation via multipolar forces. This would wash out the dip at line center. However, this phenomenological approach is somewhat misleading in treating collision-induced electronic spectral lines because short-range intermolecular forces will not just couple to the dipole moment operator of the atom. Consequently, the collision-induced transient dipole moment for collisions less than the hard-core impart parameter will no longer involve just the Raman scattering tensor, and the entire formulation of Sec. II cannot be applied to this regime. Instead, we prefer to treat only the contribution arising from the long-range electrostatic potential and reserve for future publication the contribution of short-range intermolecular interactions on collision-induced electronic transitions. Thus, Fig. 4 is the line shape determined solely by long-range ion-atom forces.

The relatively narrow widths of the ion-atom, collision-induced absorption lines reflect the long lifetime

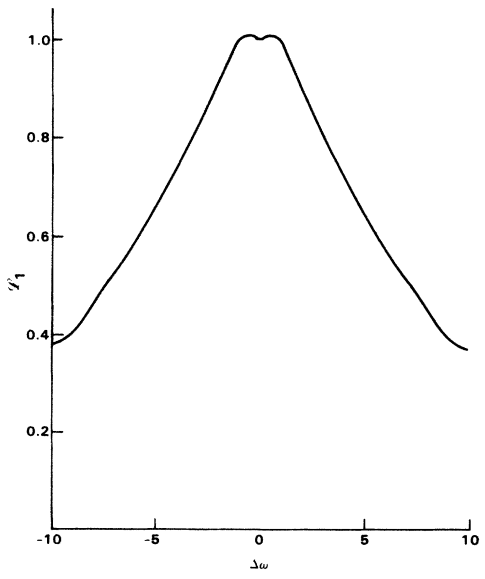

FIG. 4. Line shape of ion-atom collision-induced absorption.

of the CI transient electric dipole induced by the ion's electric field. In particular, the CI dipole moment in real time is, neglecting anisotropic features,

$$\mu^{i\to f}(t) \simeq \tfrac{1}{2}(4\pi/3)^{3/2}(Ze/b^2) \times C_k^{i\to f}(J_i,J_p)\frac{e^{-i\omega_{if}t}}{[1+(vt/b)^2]} . \tag{3.3}$$

Typical values of the CI dipole are 1 D for $b \approx 10$ Å at the point of closest approach. This will fall to 0.01 D for times $t = 10b/v \approx 10^{-10}$ s for relative velocities on the order of 10^4 cm/s. Thus typical lifetimes for ion-atom, collision-induced dipoles are on the order of 10—100 ps, which is considerably longer than occurs in standard collision-induced processes which arise in collisions involving symmetrical atoms and molecules alone. Furthermore, the symmetrical nature of the line shape is due to the fact that the relative velocity suffers only small changes during most of the emission process. In contrast, collision-induced processes occurring via short-range forces are characterized by significant changes in velocity which in turn give rise to very asymmetric line shapes. The rapid drop of the collision-induced line shape is analogous to the sharp energy dependence of inelastic rotational and rotovibrational cross sections that proceed via long-range electrostatic forces.

To obtain the collision-induced spontaneous emission rate A for ion-atom processes we note that the total cross section for collision-induced emission is, from Eq. (2.9),

$$\sigma_{i\to f} \cong \frac{(8\pi)^2}{27}(Ze)^2\frac{c}{v_T^2}Q_R(\omega_{if},0)\left[\ln\left[\frac{\lambda_D}{b^*}\right]\right]\Delta\omega^* , \tag{3.4}$$

where the frequency integration was approximated as the cross section for collision-induced emission processes at line center times the line width. Finally, the CI spontaneous emission rate $A = n_p v_T \sigma_{i\to f}$,

$$A = \frac{(8\pi)^2}{27}(Ze)^2\frac{c}{v_T}\left[\ln\left[\frac{\lambda_D}{b^*}\right]\right]Q_R(\omega,0)n_p\Delta\omega^* , \tag{3.5}$$

which is independent of collision velocity since $\Delta\omega^*$ is directly proportional to v_T.

Next, we estimate the magnitude of the collision-induced absorption coefficient at line center for the $^3P_0 \to 1S_0$ transition of Sn. The $^3P_0 \to {}^1S_0$ transition of Sn occurs at 17 163 cm^{-1} and the two levels in question are strongly coupled to the $^3D_1$ (at 44 509 cm^{-1}) and $^3P_1$ (at 39 257 cm^{-1}) levels. For this transition $Q_R \simeq 6\times 10^{-15}$ esu and $\lambda = 0.58$ μm. We find an absorption coefficient of 0.45%/cm $torr^{-1}$ of Sn was found at $T \simeq 300$ K for 0.1 torr of Cs^+ and $b^* = 3$ Å.

At a distance of 10 Å the total probability for a collision-induced event is about 0.51×10^{-5} so that the Born approximation should be fairly accurate. The cross section for collision-induced spontaneous emission is about 2.15×10^{-2} Å^2 and the spontaneous emission radiative lifetime is about 5.22×10^{-3} s, which implies a radiative rate of 191.52 s^{-1}.

2. Beam configuration

In this subsection we again consider ion-atom collision-induced absorption processes, but in this case the perturbers and atoms collide in a beam configuration. The line shape of the collision-induced absorption spectra will sensitively reflect the spatial configuration of the colliding particles. This feature of ion-atom collision-induced processes arises from the anisotropic nature of the ion-atom interaction. As a result of the beam configuration, line-shape effects due to collision-induced absorption processes mediated via short-range intermolecular forces should be much more apparent than the situation discussed in Sec. III A 1. Accordingly, this may enable one to isolate the influence of short-range interactions on collision-induced electronic transitions, as the theory presented here includes only long-range forces. Since we are examining a beam situation, the derivation presented in Sec. II, which sums over all directions, is not applicable to the present problem. Instead, we start with Eq. (2.12) for the collision-induced dipole moment for structureless perturbers. Thus,

$$p_{m_3}^{i\to f}(t)=\sum_n \left[\frac{\langle f\,|\,\mu^1_{m_3}\,|\,n\rangle\langle n\,|\,V_1(t)\,|\,i\rangle}{\hbar\omega_{ni}} + \frac{\langle f\,|\,V_1(t)\,|\,n\rangle\langle n\,|\,\mu^1_{m_3}\,|\,i\rangle}{\hbar\omega_{nf}} \right] e^{-i\omega_{if}t}, \tag{3.6}$$

where

$$V_1(t)=\frac{Ze}{R^2(t)}\hat{\mathbf{R}}(t)\cdot\boldsymbol{\mu} \tag{3.7}$$

is the ion-atom potential. Denoting the atomic states by $|nJM\rangle$ gives

$$p_{m_3}^{i\to f}(t)=\frac{Ze}{R^2(t)}\hat{\mathbf{R}}(t)\cdot\mathbf{C}_{m_3}e^{i\omega_{if}t} \tag{3.8}$$

with

$$\mathbf{C}_{m_3}\equiv\sum_{nJM}\left[\frac{\langle n_i00\,|\,\mu^1_{m_3}\,|\,nJM\rangle\langle nJM\,|\,\boldsymbol{\mu}^1\,|\,n_f00\rangle}{\hbar\omega_{ni}} + \frac{\langle n_i00\,|\,\boldsymbol{\mu}^1\,|\,nJM\rangle\langle nJM\,|\,\mu^1_{m_3}\,|\,n_f00\rangle}{\hbar\omega_{nf}} \right] \tag{3.9}$$

the projection of the Raman scattering tensor onto the m_3 direction. An examination of Eq. (3.9) reveals three components,[18]

$$C_{00}=\sum_n \langle n_i00\,|\,\mu^1_0\,|\,n10\rangle\langle n_i10\,|\,\mu^1_0\,|\,n_f00\rangle\frac{\omega_{ni}+\omega_{nf}}{\hbar\omega_{ni}}, \tag{3.10}$$

$$C_{+,-}=\sum_n \left[\frac{\langle n_i00\,|\,\mu^1_+\,|\,n1-1\rangle\langle n1-1\,|\,\mu^1_-\,|\,n_f00\rangle}{\hbar\omega_{ni}} + \frac{\langle n_i00\,|\,\mu^1_-\,|\,n11\rangle\langle n11\,|\,\mu^1_+\,|\,n_f00\rangle}{\hbar\omega_{nf}} \right], \tag{3.11}$$

$$C_{-,+}=(C_{+,-})^*, \tag{3.12}$$

and using

$$\hat{\mathbf{e}}_z\cdot\hat{\mathbf{e}}_z=1,\quad \hat{\mathbf{e}}_2\cdot\hat{\mathbf{e}}_\pm=0,\quad \hat{\mathbf{e}}_\pm\cdot\hat{\mathbf{e}}_\mp=1,\quad \hat{\mathbf{e}}_\pm\cdot\hat{\mathbf{e}}_\pm=0 \tag{3.13}$$

we have, for the various components of the collision-induced transition electric dipole,

$$p_z^{i\to f}(t)=\frac{Ze}{R^2(t)}C_{00}[\hat{\mathbf{R}}(t)\cdot\hat{\mathbf{e}}_z]e^{-i\omega_{if}t}, \tag{3.14a}$$

$$p_+^{i\to f}(t)=\frac{Ze}{R^2(t)}C_{+,-}[\hat{\mathbf{R}}(t)\cdot\hat{\mathbf{e}}_+]e^{-i\omega_{if}t}, \tag{3.14b}$$

$$p_-^{i\to f}(t)=\frac{Ze}{R^2(t)}C_{-,+}[\hat{\mathbf{R}}(t)\cdot\hat{\mathbf{e}}_-]e^{-i\omega_{if}t}. \tag{3.14c}$$

To appreciate the role of anisotropy, we consider two separate situations: (1) parallel beams and (2) perpendicular beams.

3. Parallel beams

If the relative velocity vector $\mathbf{v}$ defines the $\hat{\mathbf{e}}_z$ axis, we have

$$p_z^{i\to f}(t)=\frac{Ze}{R^2(t)}C_{00}\frac{vt}{R(t)}e^{-i\omega_{if}t}, \tag{3.15a}$$

$$p_+^{i\to f}(t)=\frac{Ze}{R^2(t)}C_{+,-}\frac{b_-}{R(t)}e^{-i\omega_{if}t}, \tag{3.15b}$$

$$p_-^{i\to f}(t)=\frac{Ze}{R^2(t)}C_{-,+}\frac{b_+}{R(t)}e^{-i\omega_{if}t}. \tag{3.15c}$$

An examination of Eqs. (3.15) reveals that $p_z^{i\to f}(t)$ is an odd function of time and $p_\pm^{i\to f}(t)$ are even. This implies that $p_z^{i\to f}(\omega)$ is zero on resonance. In particular,

$$p_z^{i\to f}(\omega)=i\frac{ZeC_{00}}{v^2}\Delta\omega K_0\left[\frac{\Delta\omega b}{v}\right], \tag{3.16a}$$

$$p_+^{i\to f}(\omega)=\frac{ZeC_{+,-}}{v^2}\frac{b_+}{b}\Delta\omega K_1\left[\frac{\Delta\omega b}{v}\right], \tag{3.16b}$$

$$p_-^{i\to f}(\omega)=p_+^{i\to f}(\omega)^*. \tag{3.16c}$$

Thus, as $\Delta\omega\to 0$,

$$p_z^{i\to f}(\omega)\to -i\frac{ZeC_{00}}{vb}\left[\frac{\Delta\omega b}{v}\right]\ln\left[\frac{\Delta\omega b}{v}\right], \tag{3.17a}$$

$$p_+^{i\to f}(\omega)\to\frac{ZeC_{+,-}}{vb}, \tag{3.17b}$$

$$p_-^{i\to f}(\omega)\to\frac{ZeC_{-,+}}{vb}, \tag{3.17c}$$

i.e., the component of the dipole moment in the z direc-

tion vanishes almost linearly with $\Delta\omega$ as $\omega\rightarrow\omega_{if}$. On the other hand, $p_{\pm}^{i\rightarrow f}(\omega)$ approach a constant. Thus, if I_n denotes the radiation intensity in the direction n,

$$I_z(\omega)\underset{\omega\rightarrow\omega_{if}}{\rightarrow}\frac{4\pi\omega_{if}^4}{3c^3}|C_{+-}|^2\frac{c}{v}(Ze)\ln\left[\frac{\lambda_D}{b^*}\right]n_pN\ , \quad (3.18a)$$

$$I_x(\omega)=I_y(\omega)\rightarrow\frac{2\pi\omega_{if}^4}{3c^3}\frac{c}{v}Ze|C_{+-}|^2\ln\left[\frac{\lambda_D}{b^*}\right]n_pN\ , \quad (3.18b)$$

where we have used the fact that $|C_{+-}|=|C_{-+}|$. Note that only plane-polarized radiation is absorbed since $\Delta M=0$. Note, too, that the influence of short-range interactions on collision-induced transitions should be apparent from the deviation of the ratio $I_x/I_z=I_y/I_z=0.5$ near line center.

4. Crossed beams

Let the impact parameter **b** define the $\hat{\mathbf{e}}_z$ axis; then

$$p_z^{i\rightarrow f}(t)=\frac{Ze}{R^2(t)}C_{00}\frac{b}{R(t)}e^{-i\omega_{if}t}\ , \quad (3.19a)$$

$$p_+^{i\rightarrow f}(t)=\frac{Ze}{R^2(t)}C_{+,-}\frac{v_-t}{R(t)}e^{-i\omega_{if}t}\ , \quad (3.19b)$$

$$p_-^{i\rightarrow f}(t)=\frac{Ze}{R^2(t)}C_{-,+}\frac{v_+t}{R(t)}e^{-i\omega_{if}t}\ . \quad (3.19c)$$

Thus,

$$p_z^{i\rightarrow f}(\omega)=\frac{ZeC_{00}}{vb}\left[\frac{\Delta\omega b}{v}\right]K_1\left[\frac{\Delta\omega b}{v}\right]\ , \quad (3.20a)$$

$$p_+^{i\rightarrow f}(\omega)=-i\frac{ZeC_{+,-}}{vb}\frac{v_-}{v}\left[\frac{\Delta\omega b}{v}\right]K_0\left[\frac{\Delta\omega b}{v}\right]\ , \quad (3.20b)$$

$$p_-^{i\rightarrow f}(\omega)=-i\frac{ZeC_{-,+}}{vb}\frac{v_+}{v}\left[\frac{\Delta\omega b}{v}\right]K_0\left[\frac{\Delta\omega b}{v}\right]\ ; \quad (3.20c)$$

only the component of the dipole moment which is normal to the plane defined by the beams is nonzero on resonance. This implies that no resonant collision-induced radiation is emitted normal to the plane of the beams, i.e.,

$$I_z(\omega_{if})=0\ , \quad (3.21a)$$

$$I_x(\omega_{if})=I_y(\omega_{if})=\frac{2\pi\omega_{if}^4}{3c^3}\frac{c}{v}Ze\left[\ln\left[\frac{\lambda_D}{b^*}\right]\right]n_pN\ . \quad (3.21b)$$

The contribution of short-range forces will be apparent if one observes the radiation emitted in the plane of the collision.

B. Molecular dipoles

We consider a gas of atoms and molecular dipole perturbers in thermodynamic equilibrium at a temperature T and confine ourselves to collision-induced electric dipole transitions in which only the rotational state of the perturber changes. The interaction is thus dipole dipole, and Fig. 5 depicts the resonance function versus $\Delta\omega b/v$. An

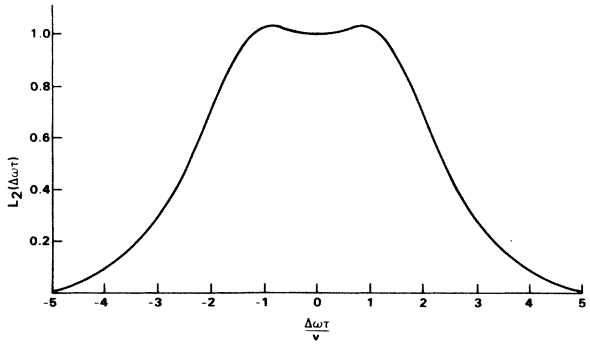

FIG. 5. First-order resonance function for molecular dipole-atom forces.

examination of this figure reveals a well-defined dip at line center, arising from the anisotropic nature of the molecular dipole-atom interaction. Note that the width of the resonance function is somewhat greater than the ion-atom case due to the fact that dipole-atom forces decrease with distance more rapidly than ion-atom forces. Furthermore, for collision-induced processes in which an atom spontaneously emits a photon while the perturber goes from the state $J\rightarrow J+1$, the CI spontaneous emission rate is

$$\mathscr{A}_2(\omega)=\frac{32\pi^3}{729}P^2\left[\frac{J+1}{2J+1}\right]\frac{Q_R(\omega_{if},-2B(J+1))}{\sigma_{\rm hc}}\frac{c}{v_T}$$

$$\times n_p(J)\mathscr{L}_2(\omega-\omega_{if}+2B(J+1),T)\ , \quad (3.22)$$

where $\sigma_{\rm hc}$ is the hard-core cross section, P is the dipole moment of the perturber, and $n_p(J)$ is the density of molecules in the rotational state J. For spontaneous emission processes in which the perturber goes from $J\rightarrow J-1$,

$$\mathscr{A}_2(\omega)=\frac{32\pi^3}{729}P^2\left[\frac{J}{2J+1}\right]\frac{c}{v_T}\frac{Q_R(\omega_{if},2BJ)}{\sigma_{\rm hc}}$$

$$\times n_p(J)\mathscr{L}_2(\omega-\omega_{if}-2BJ,T)\ . \quad (3.23)$$

Thus, each molecular state J will give rise to two collision-induced spontaneous emission lines centered at $\omega=\omega_{if}-2B(J+1)$ and $\omega=\omega_{if}+2BJ$ with relative strengths of $(J+1)/J$. Since the perturbers themselves are in a Boltzmann distribution, a manifold of collision-induced spontaneous emission lines will appear centered at $\omega=\omega_{if},\omega_{if}\pm2B,\omega_{if}\pm4B,\omega_{if}\pm6B,\ldots$. The relative intensity of two neighboring lines $S(J)$ [i.e., $\omega_{if}-2BJ$ and $\omega_{if}+2B(J-1)$] are, on resonance,

$$S(J)=\frac{J^2}{J^2-1}e^{-2\hbar BJ/k_BT},\quad J=2,3,\ldots\ . \quad (3.24)$$

A similar expression can be constructed for the lines centered at $\omega_{if}-2B(J+1)$ and $\omega_{if}-2BJ$. If the rotation constant $B\leq v_T/b^*$, then the various collision-induced spectral lines will overlap with one another and the resultant spectrum can be quite complex.

If the metastable atoms are all in the ground state, then

the collision-induced absorption coefficient is

$$\alpha_2(\omega)=\frac{4\pi^2}{81}(P\lambda)^2\left[\frac{J+1}{2J+1}\right]\frac{c}{v_T}\frac{Q_R(\omega_{if},2BJ)}{\sigma_{hc}}$$

$$\times\mathscr{L}_2(\omega-\omega_{if}+2B(J+1),T)n_p(J)N \tag{3.25}$$

for processes in which the perturber goes from $J\rightarrow J+1$ and

$$\alpha_2(\omega)=\frac{4\pi^2}{81}(P\lambda)^2\left[\frac{J}{2J+1}\right]\frac{c}{v_T}\frac{Q_R(\omega_{if},2B(J+1))}{\sigma_{hc}}$$

$$\times\mathscr{L}_2(\omega-\omega_{if}-2B(J+1),T)n_p(J)N \tag{3.26}$$

for processes in which $J\rightarrow J-1$.

Next, consider the detailed line shape of the collision-induced spectral lines for nonoverlapping lines. Figure 6 depicts the case of Sn and DF (deuterium fluoride) at 300 K with a hard-core impact parameter of 3 Å. Since the rotation constant for DF (deuterium fluoride) is 20 cm^{-1}, the centers of the different CI spectral lines are separated by about 40 cm^{-1}. As the collision-induced absorption linewidths are on the order of v_T/b, where b is a typical impact parameter, the FWHM is about 20 cm^{-1}. Thus, to good approximation, one can regard each spectral line separately. The line-shape function has the following characteristics: (1) It is relatively narrow with a FWHM linewidth of about 18 cm^{-1}; (2) it is symmetrical about the line center; (3) for $\Delta\omega\gg v/b^*$ it declines exponentially, in fact, as $\exp(-\Delta\omega b^*/v)$; and (4) its shape and width are independent of gas pressure. As in the ion-induced spectra, the dip at line center should be washed out by collision-induced processes due to short-range forces. We comment upon the physics of these features below.

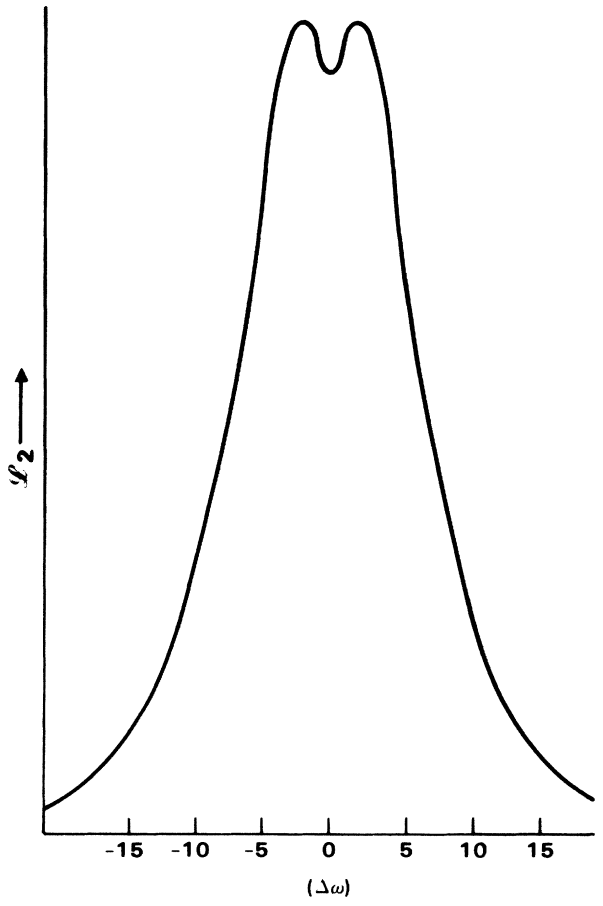

FIG. 6. Line shape for an isolated atom-molecular dipole collision-induced spectral.

As in ion-atom CI absorption, the relatively narrow widths of these collision-induced absorption lines reflect the long lifetime of the transient CI electric dipole induced by the presence of the perturber. In particular, the collision-induced dipole moment in real time is

$$\mu^{i\rightarrow f}(t)\cong\frac{1}{2}\left[\frac{4\pi}{3}\right]^{3/2}(P/b^3)C_k^{i\rightarrow f}(J_i,J_f)$$

$$\times\frac{e^{-i\omega_{if}t}}{[1+(vt/b)^2]^{3/2}}\,, \tag{3.27}$$

where we have neglected the orientational dependence of the atom-molecular dipole interaction for simplicity. Typical values of the collision-induced electric dipole moment at 10 Å are 0.1 D with DF as perturber. This will fall to 0.01 D for times $t\sim 3b/v\sim 3\times 10^{-10}$ s for relative velocities on the order of 10^4 cm/s. Thus, typical lifetimes for molecular dipole-atom, collision-induced electric dipoles are about 10 ps which is considerably longer than standard collision-induced processes involving short-range forces. As in the ion-atom case the symmetrical nature of the line shape is due to the fact that the relative velocity suffers only small changes during most of the radiation process. In contrast, collision-induced processes occurring via short-range forces are characterized by significant changes in velocity which in turn give rise to very asymmetric line shapes. The relatively rapid drop of the collision-induced line shape is analogous to the sharp energy dependence of inelastic rotational and rotovibrational cross sections that proceed via long-range electrostatic forces.[12] As noted previously, the width of the induced spectral line is approximately $(\hbar w_T/b^*)$ which is much broader than collision-induced widths that occur for most gases operating at standard pressures. Thus, the collision-induced linewidth will remain constant with increasing gas densities as long as $(\hbar w_T/b^*)$ exceeds the collision-broadened widths which should not occur until gas pressures are on the order of tens of atmospheres.

Next, the magnitude of the collision-induced absorption line on line center is estimated. Now consider the $^3P_0\rightarrow{}^1S_0$ Sn transition using DF as perturber at 300 K. As noted in Eq. (3.1), for this transition $Q_R\simeq 6\times 10^{-15}$ esu and $\lambda=0.58$ μm. For DF, $P=1.83$ D, and choosing $b^*=3$ Å results in $\alpha_2(0)=(2.5\times 10^{-3}$ %/cm)/(torr of Sn)(torr of DF) in a particular rotational state. Thus, if a single torr of Sn is vaporized in the presence of DF, the collision-induced absorption coefficient on line center for $J\sim k_BT/\hbar B$ is about 0.1%/cm per atmosphere of DF.

IV. DISCUSSION AND CONCLUSION

In this paper we have examined collision-induced radiative processes arising from long-range electrostatic forces. Below we summarize our findings.

If an atom collides with an ion or molecule, which is characterized by an electric multipole moment of order l_1, it will acquire a CI transition electric dipole moment $p_{m_3}^{i\to f}(t)$ given by

$$p_{m_3}^{i\to f}(t)=-\frac{4\pi}{2l+1}\left[\frac{4\pi(2l+1)!}{3(2l_1+1)!}\right]^{1/2}\times\sum_{\substack{m,m_1\\ m_2}}\langle m_1 m_2\,|\,lm\rangle\langle a\,|\,\mu_{m_1}^{l_1}\,|\,c\rangle\times C_{m_2 m_3}^{i\to f}\frac{Y_{lm}^{*}[\hat{\mathbf{R}}(t)]}{R^{l+1}(t)}e^{-i(\omega_{if}+\omega_{ac})t}, \tag{4.1}$$

where $l=l_1+1$, $\mathbf{R}(t)$ is the classical path of the relative coordinate, $C_{m_1 m_3}^{i\to f}$ is the relevant Raman scattering tensor, $\langle a\,|\,\mu_{m_1}^{l_1}\,|\,c\rangle$ is the allowed matrix element of the l_1 electric multipole moment the states $|a\rangle$ and $|c\rangle$ of the perturber, and $|i\rangle$ ($|f\rangle$) is the initial (final) state of the atom, the transition $|i\rangle\to|f\rangle$ being forbidden in the absence of the perturber. The collision-induced dipole moment oscillates at a frequency $\omega_{if}+\omega_{ac}$, the shift arising from the fact that the perturber has undergone an allowed transition $|a\rangle\to|c\rangle$. The transient nature of the collision-induced dipole moment is reflected in the time dependence of the relative coordinate $\mathbf{R}(t)$. If the classical path can be approximated as a linear trajectory, i.e.,

$$R^2(t)=b^2+v^2t^2\,, \tag{4.2}$$

where b is the impact parameter and v the relative velocity, then the lifetime of the collision-induced dipole is set by b/v. An examination of Eq. (4.1) reveals that the higher the order of the perturber's electric multipole moment, the shorter the lifetime of the induced dipole. This feature is entirely reasonable as it merely reflects the fact that the electric field associated with an electric multipole of order l_1 varies as $1/R^{l+1}$. The presence of the spherical harmonic, $Y_{lm}^{*}[\hat{\mathbf{R}}(t)]$ in Eq. (4.1), arises from the anisotropic nature of long-range electrostatic forces. The influence of this anisotropy on the collision-induced dipole moment can be appreciated most readily by specializing to the case of ion-atom collisions which are prepared in a parallel-beam configuration. The component of the collision-induced dipole which is parallel to the beam axis is

$$p_z^{i\to f}(t)=ZeC_{00}\frac{vt}{R^3(t)}e^{-i\omega_{if}t}\,, \tag{4.3a}$$

whereas the components which are normal to the beam direction are

$$p_{\pm}^{i\to f}(t)=ZeC_{\pm,\mp}\frac{b_{\pm}}{R^3(t)}e^{-i\omega_{if}t} \tag{4.3b}$$

with $b_{\pm}=\mathbf{b}\cdot\hat{\mathbf{e}}_{\pm}$. An examination of Eqs. (4.3) reveals that the various components of the collision-induced electric dipole moment differ in both magnitude and temporal behavior. Thus, the component parallel to the beam axis is zero at the point of closest approach, peaks at $t=b/v$, and decays to zero as

$$p_z^{i\to f}(t)\underset{t\to\infty}{\to}\frac{ZeC_{00}}{(vt)^2}e^{-i\omega_{if}t}\,. \tag{4.4}$$

In contrast, the component normal to the beam direction peaks at the point of closest approach and decays to zero more rapidly:

$$p_{\pm}^{i\to f}(t)\underset{t\to\infty}{\to}\frac{ZeC_{\pm,\mp}}{(vt)^2}\left[\frac{b_{\pm}}{vt}\right]e^{-i\omega_{if}t}\,. \tag{4.5}$$

Further examination of Eq. (4.1) reveals that all of the electronic structure of the atom is contained in the Raman scattering tensor, $C_{m_2 m_3}^{i\to f}$. The presence of the Raman scattering tensor in the collision-induced transient electric dipole is to be expected as its reflects the fact that the atom acquires its CI electric dipole moment via a Raman-like process. In particular, the electric field of the perturber polarizes the electronic structure of the atom. This process can be viewed as one in which the atom, initially in the state $|i\rangle$, is virtually excited to an intermediate state $|n\rangle$ and then makes a transition to the state $|f\rangle$ with the emission (or absorption) of a photon whose frequency is close to ω_{if}. In all cases the transition is mediated by the allowed transition electric dipole moments of the atom. The quasistatic nature of the excitation process is reflected in the nonresonant denominators of $C_{m_2 m_3}^{i\to f}$.

The Raman scattering tensor can be decomposed into three irreducible pieces, i.e., a scalar for which $\Delta J=0$, an antisymmetric tensor of rank two for $\Delta J=1$ processes, and a symmetric tensor of rank two for $\Delta J=2$. Of these, the smallest is $\Delta J=1$ so that the collision-induced electric dipole would be the smallest for spin-orbit magnetic-dipole-type processes, e.g., the $^2P_{1/2}\to{}^2P_{3/2}$ transition in atomic iodine. On the other hand, $\Delta J=0$ and $\Delta J=2$ processes have much larger Raman cross sections and are much more promising candidates for observing significant collision-induced absorption and emission utilizing long-range electrostatic fields, in particular the $^3P_0\to{}^1S_0$ and $^3P_2\to{}^1S_0$ Sn transitions. Additional interesting transitions are the $^3P_2\to{}^1S_0$ of Xe and other heavy rare gases.

If a gas of atoms is prepared in the ground state, then the collision-induced absorption coefficient on a forbidden electronic transition in the presence of a spatially homogeneous electron-ion plasma is

$$\alpha_1(\omega)=\frac{8\pi}{27}(Ze\lambda)^2\frac{c}{v_T}Q_R(\omega_{if},0)\times[\ln(\lambda_D/b^*)]\mathscr{L}_1(\Delta\omega,T)n_p N\,, \tag{4.6}$$

where v_T is the thermal velocity of the perturber-atom pair, λ_D is the Debye wavelength of the plasma, b^* is the hard-core impact parameter, Ze is the ion charge, $\lambda(\omega)$ is

the photon wavelength (frequency), n_p is the ion density, N is the atomic density,

$$Q_R = \frac{\partial}{\partial \omega'} \sigma_R^{i \to f}(\omega_{if}, \omega') \Big|_{\omega'=0} , \tag{4.7}$$

where $\sigma_R^{i \to f}(\omega_{if}, \omega')$ is the Raman cross section, and $\mathscr{L}_1(\Delta\omega, T)$ is the line shape of the collision-induced spectral line which is normalized to unity on resonance. Several features of Eq. (4.6) should be discussed.

The logarithmic factor $\ln(\lambda_D / b^*)$ arises from and reflects the long-range nature of ion-atom, collision-induced transition electric dipole moments. Specifically, the Fourier transform of Eq. (4.1) on resonance is

$$p_{m_3}^{i \to f}(\omega_{if}) = \frac{16\pi}{3} i \left(\frac{Ze}{bv} \right) \sum_{m_2} \langle 0 m_2 \mid 11 \rangle C_{m_2 m_3}^{i \to f} \tag{4.8}$$

which varies inversely with impact parameter. It follows that since the collision-induced absorption coefficient involves

$$\alpha_1(\omega) \sim \int db \frac{1}{b} \sim \ln b , \tag{4.9}$$

it will diverge as $b \to \infty$. The cutoff, introduced in Eq. (4.9), simulates screening arising from the collective behavior of the plasma. Since screening enters into the induced absorption coefficient logarithmatically, it does not strongly influence the magnitude of $\alpha_1(\omega)$. The velocity ratio c/v_T implies that the collision-induced absorption coefficient is greatest at lowest collision velocities. Hence, one prefers to use heavy perturbers and atoms as well as low temperatures to maximize the effect. The presence of a spatially homogeneous, neutral electron-ion plasma generally implies relatively high temperatures so that it is important to use heavy particles in examining these effects. Low collision velocities may be achieved by utilizing merging ion and atomic beams instead of a homogeneous plasma and gas. However, merging-beam technology is somewhat immature with relatively low densities presently available. Note, too, that to ensure a neutral plasma, the interaction region will have to be irradiated with an electron beam.

The line-shape factor in Eq. (4.6) exhibits a dip at line center and peaks at $\Delta\omega \cong \pm v_T / b^*$ followed by an exponential decline for $|\Delta\omega| \gg v_T / b$. As mentioned previously, the dip at line center should be washed out by collision-induced processes due to short-range interactions. Thus, the precise shape of the line near line center will also depend upon details of the short-range intramolecular forces and will be discussed elsewhere. The width of the collision-induced spectral line is set by v_T / b^* and is entirely independent of gas density. This feature of the collision-induced radiative process is due to the fact that the lifetime of the collision-induced dipole is set by the duration of the collision and not by the time between collisions. Thus, the linewidth of the collision-induced spectral line is independent of pressure at least until gas densities n are such that $\tau_C = [1/(n v_T \sigma)^{1/2}] \sim b^* / v_T$, with σ the cross section for ion-atom collisions. This should not occur until n is on the order of several tens of atmospheres.

If molecular dipoles are utilized as perturbers, the induced absorption coefficient is given by

$$\alpha_1(\omega) = \frac{4\pi^2}{81} (P\lambda)^2 h_J \frac{c}{v_T} \frac{Q_R(\omega_{if}, 2B(J+1))}{\sigma_{hc}} \times \mathscr{L}_2(\Delta\omega, T) n_p(J) N , \tag{4.10}$$

where P is the rotational dipole moment of the perturber, $\sigma_{hc} = \pi (b^*)^2$ is the hard-core cross section, $\mathscr{L}_2(\Delta\omega, T)$ is the line shape, $n_p(J)$ is the perturber density in the rotational state J, and

$$h_J = \begin{cases} (J+1)/(2J+1) & \text{if } J \to J+1 \\ J/2+1 & \text{if } J \to J-1 \end{cases}$$

which is about one-half. In general, $\alpha_2(\omega)$ has the same basic features as $\alpha_1(\omega)$ except that it is smaller and somewhat broader.

APPENDIX: DERIVATION OF THE COLLISION-INDUCED OPTICAL STRENGTH FUNCTION

In this appendix we derive Eq. (2.21) for the collision-induced optical strength function

$$S_l(\Delta\omega, b, v) \equiv B_l^2(v,b) \sum_{m_3} \sum_{\substack{m' m_1' \\ m_2'}} \sum_{\substack{m m_1 \\ m_2}} \langle m_1 m_2 \mid l m \rangle \langle m_1' m_2' \mid l m' \rangle \langle a \mid \mu_{m_1}^{l_1} \mid c \rangle \langle a \mid \mu_{m_1'}^{l_1} \mid c \rangle^* \times C_{m_2 m_3}^{i \to f} C_{m_2' m_3}^{i \to f *} f_{l,m}(\Delta\omega b / v) f_{l,m'}(\Delta\omega b / v)^* . \tag{A1}$$

We first note that

$$\langle a \mid \mu_{m_1}^{l_1} \mid c \rangle = \langle n_p Q_{l_1} \mid n_p' \rangle \langle J M_p \mid Y_{l_1 m_1}(\hat{\mathbf{r}}_1) \mid J_p' M_p' \rangle = \langle n \mid Q_{l_1} \mid n' \rangle \begin{bmatrix} J_p & l_1 & J_p' \\ -M_p & m_1 & M_p' \end{bmatrix} , \tag{A2}$$

where

$$\begin{bmatrix} J & l_1 & J' \\ -M & m_1 & M \end{bmatrix}$$

is a Wigner $3j$ coefficient, i.e., a matrix element of a spherical harmonic. Furthermore,

$$\overline{\begin{pmatrix} J_p & l_1 & J_p' \\ -M_p & m_1 & M_p' \end{pmatrix}\begin{pmatrix} J_p & l_1 & J_p' \\ -M_p & m_1' & M_p' \end{pmatrix}} = \frac{\delta_{m_1 m_1'}}{2l_1+1}\delta(J_p J_p' l_1) , \tag{A3}$$

where $\delta(JJ'l_1)=1$ if J,J',l_1 satisfy the triangular condition, $|J-J'|=l_1$, and is zero otherwise. Combining Eqs. (A2) and (A3), we find

$$\overline{\langle a|\mu_{m_1}^{l_1}|c\rangle\langle a|\mu_{m_1}^{l_1}|c\rangle^*} = \frac{\overline{|\langle n_p J_p|Q_{l_1}|n_p' J_p'\rangle|^2}}{2l_1+1}\delta_{m_1 m_1'} , \tag{A4}$$

where $|\mathbf{J}-\mathbf{J}'|=l_1$. Inserting Eqs. (A4) into Eq. (A1) we have

$$S_l(\Delta\omega,b,v) = \frac{B_l^2(v,b)\,\overline{|\langle n_p J_p|Q_{l_1}|n_p' J_p'\rangle|^2}}{2l_1+1} \times \sum_{m_3}\sum_{\substack{m_1 m_2 \\ m}}\sum_{\substack{m_2' \\ m'}} \langle m_1 m_2|lm\rangle\langle m_1 m_2'|lm'\rangle^* C_{m_2 m_3}^{i\to f} C_{m_2' m_3}^{i\to f\,*} f_{l,m}(\Delta\omega b/v) f_{l,m'}(\Delta\omega b/v)^* . \tag{A5}$$

Next, the scattering tensor $C_{m_2 m_3}^{i\to f}$ is decomposed into its irreducible pieces, so that

$$\overline{C_{m_2 m_3}^{i\to f} C_{m_2' m_3}^{i\to f}} = \sum_{kq}\langle m_2 m_3|kq\rangle\langle m_2' m_3|kq\rangle \frac{|(n_i J_i||T^{(k)}||n_f J_f)|^2}{(2J_i+1)(2k+1)} , \tag{A6}$$

where $(n_i J_i||T^{(k)}||n_f J_f)$ is the irreducible scattering tensor of order k and J_i,J_f,k satisfy the triangle condition. To evaluate Eqs. (A5) and (A6), note that

$$\sum_{q,m_3}\langle m_2 m_3|kq\rangle\langle m_2 m_3'|kq\rangle = \delta_{m_2,m_2'} , \tag{A7}$$

$$\sum_{m_1 m_2}\langle m_1 m_2|l_1 m\rangle\langle m_1 m_2|lm'\rangle = \delta_{m,m'} , \tag{A8}$$

and

$$S_l(\Delta\omega,b,v) = \frac{B_l^2(v,b)\,|\langle n_p J_p|Q_{l_1}|n_p' J_p'\rangle|^2\,|(n_i J_i||T^{(k)}||n_f J_f)|^2}{(2l_1+1)(2J_i+1)(2k+1)} , \tag{A9}$$

where

$$L_l(\Delta\omega b/v) \equiv \sum_m |f_{l,m}(\Delta\omega b/v)|^2 \tag{A10}$$

is the first-order resonance function which determines the behavior of near-resonant, rotational multipole collisions.

[1]Proceedings of the Conference on Collision-Induced Phenomena: Absorption Light Scattering and Static Properties (Firenze, Italy, 1980) [Can J. Phys. **59**, 1403 (1981)].

[2]*Intermolecular Spectroscopy and Dynamical Properties of Dense Systems, Proceedings of the International School of Physics, "Enrico Fermi," Course LXXV,* edited by J. Van Kranendock (North-Holland, Amsterdam, 1980).

[3]H. L. Welsh, in *Physical Chemistry,* Vol. 3 of *International Review of Science,* edited by D. A. Ramsay (Butterworths, London, 1973).

[4]Z. J. Kiss, H. P. Gush, and H. L. Welsh, Can. J. Phys. **37**, 362 (1959).

[5]D. R. Bosomworth and H. P. Gush, Can. J. Phys. **43**, 729 (1965).

[6]Z. J. Kiss and H. L. Welsh, Can. J. Phys. **37**, 1249 (1959).

[7]W. F. J. Hare and H. L. Welsh, Can. J. Phys. **36**, 88 (1958).

[8]G. Varghese and S. P. Reddy, Can. J. Phys. **47**, 2745 (1969).

[9]J. D. Poll and J. L. Hunt, Can. J. Phys. **63**, 84 (1985), and references therein.

[10]D. Rogovin and P. Avizonis, Appl. Phys. Lett. **38**, 66 (1981).

[11]D. Rogovin, P. Avizonis, and J. Filcoff, Opt. Lett. **8**, 268 (1983).

[12]H. Rabitz and R. Gordon, J. Chem. Phys. **53**, 1815 (1970).

[13]D. Rogovin (unpublished).

[14]L. Landau and E. Lifshitz, *The Classical Theory of Fields* (Pergamon, Oxford, 1975).

[15]C. J. Gray, Can. J. Phys. **46**, 135 (1968).

[16]R. J. Beuhler and J. O. Herschefelder, Phys. Rev. **83**, 6238 (1951).

[17]R. D. Sharma, J. Chem. Phys. **50**, 919 (1969).

[18]V. B. Berentetskii, E. Lifshitz, and L. P. Pitaevskii, *Relativistic Quantum Mechanics* (Pergamon, Oxford, 1971).

[19]H. B. Levine and G. Birnbaum, Phys. Rev. **154**, 86 (1951).

[20]J. E. Drummond, *Plasma Physics* (McGraw-Hill, New York, 1961).